

A 3D Printing Scaffold Using Alginate/Hydroxyapatite for Application in Bone Regeneration

Bruno C. Alves^{a*}, Renato de S. Miranda^b, Barbara M. Frigieri^c, Debora A.P.C. Zuccari^d,

Marcia R. de Moura^b, Fauze A. Aouada^b, Ruis C. Tokimatsu^a

^aUniversidade Estadual Paulista, Departamento de Engenharia Mecânica, Faculdade de Engenharia de Ilha Solteira, Ilha Solteira, SP, Brasil.

^bUniversidade Estadual Paulista, Grupo de Compósitos e Nanocompósitos Híbridos, Faculdade de Engenharia de Ilha Solteira, Ilha Solteira, SP, Brasil.

^cUniversidade Estadual Paulista, Departamento de Biologia, Instituto de Biociências, Letras e Ciências Exatas, São José do Rio Preto, SP, Brasil.

^dFaculdade de Medicina de São José do Rio Preto, Departamento de Biologia Celular, São José do Rio Preto, SP, Brasil.

Received: January 16, 2023; Revised: May 24, 2023; Accepted: July 19, 2023

This work aimed to manufacture scaffolds from a hydrogel composed of a sodium alginate matrix with hydroxyapatite reinforcements using a 3D bioprinter, aiming at application in bone tissue regeneration. The alginate solution was prepared by dissolving sodium alginate at a concentration of 10% (w/v). Hydroxyapatite (HAp) was added to the solution at 2.5% and 5.0% (w/v) concentrations, followed by placing the samples in a container with a 1.0% (w/v) calcium chloride solution. The scaffolds were analyzed for HAp concentration and morphological characteristics, physicochemical properties, and biological response. The scaffolds show reproducibility and spectroscopic analyses confirm hydrogel formation and hydroxyapatite incorporation in the alginate matrix. The hydrophilic properties are compatible with scaffolds obtained through 3D printing made from polysaccharides, and the thermal analysis showed the expected behavior of these same materials. Preliminary findings indicated that scaffolds containing 2.5% (w/v) hydroxyapatite are inside cytotoxicity limit ($66.4 \pm 7.0\%$) towards canine E20 lineage cells. In contrast, scaffolds with 0% and 5.0% (w/v) hydroxyapatite were non-cytotoxic. Notably, the latter scaffold demonstrated enhanced cell proliferation, as anticipated, owing to the hydrophilic properties of alginate that enable easy and swift cell seeding, facilitating nutrient transport and cellular growth within the scaffold.

Keywords: Hydrogel, alginate, hydroxyapatite, scaffolds, biomaterials.

1. Introduction

The skeletal system is called the framework of bones and cartilage that protects our organs and allows us to move. Each bone in the skeletal system is an individual organ. This system has the functions of support, protection, movement, storage, mineral homeostasis, site of production of blood cells, and energy storage¹. Bone health directly influences the quality of life. Several factors have been increasing the demand for osteochondral repair, a defect in the cartilage of a joint and the underlying bone. Among these factors is damage related to the growing number of sports injuries, trauma from accidents, and congenital and non-congenital pathologies²⁻⁷.

Bone tissue can recover naturally under physiological conditions for millimetric damage. However, for greater extensions, natural repair does not recover the natural shape or functionally of the bone and autogenous grafts are generally the first medical option. Despite these benefits, this treatment has some limitations, such as graft availability, defect generated in the graft extraction, and the postoperative period of two injured areas^{8,9}.

In this context, bone tissue engineering emerges as a promising alternative in cases with bone loss, overcoming rejection problems and shortage of donors. Tissue engineering seeks lasting and functional solutions for bone regeneration by combining scaffolds, cells, and materials with high hydrophilic properties, which mimic the aqueous living environment. Hydrogels have been widely studied as three-dimensional (3D) matrices because they present promising systems for healing and regenerating damaged tissues precisely because they are highly permeable and facilitate the transport of nutrients and metabolites. They can mimic body tissues and respond to external stimuli, having appropriate softness and flexibility, adequate biocompatibility, biodegradability, and desirable rheological properties. These characteristics make them important and promising biomaterials for various applications, including tissue engineering and drug-release devices. Among the several materials used to manufacture scaffolds, natural polymers are the options that most attract research due to their similarities with the extracellular matrix of the tissue, biological performance, and cellular interactions¹⁰⁻¹².

*e-mail: bcrepaldialves@gmail.com

In this regard, the sodium alginate, a natural polysaccharide extracted from seaweed, pH-responsive, with biodegradable and biocompatible characteristics is a good candidate to this application. It is known to form gels in the presence of bivalent cations such as calcium ions (Ca^{2+}). Due to these characteristics, this polymer has been also widely used for depositing drugs and growth factors, cell encapsulation, and scaffolds in tissue engineering applications. However, alginate has limitations for bone tissue, such as a lack of sites for cell binding or interactions with receptor tissue, limiting its long-term functionality. Therefore, using hydroxyapatite (HAp) as a bioactive component with osteoconductive capabilities may overcome some limitations³.

HAp is commonly used in the regeneration of bone tissue due to its chemical similarity with the inorganic component of the bone matrix, biocompatibility, osteoinduction, osteoconduction, and osteointegration characteristics^{4,7}. The amount of HAp within the composition of polymer-based hydrogels is crucial to design efficient tissue for bone regeneration. Once HAp is gradually degraded, it releases Ca^{2+} and PO_4^{3-} ions, which can modify cellular behavior, influencing bone mineralization and binding to surrounding tissues. The concentration of HAp incorporated in polymer-based composites can directly influence the level of solubility, cell fixation, proliferation and differentiation, and bone growth rate^{3,13-17}.

Bone grafts have typically been performed through bone tissue transplants; however, there are several problems in using both allografts (transplantation between genetically different individuals of the same species) and autografts. These disadvantages include infections and pathogenic immune responses to the first case, the donor site's morbidity, and the limited amount of usable bone tissue for the second case¹⁸.

The restrictions described leading to the need for a safer and more reliable method that circumvents the problems with current therapeutic strategies for bone defects. 3D printing is promising as a methodology that assists in bone regeneration by mimicking the properties of mineral bone, providing bone construction and tissue growth guidelines. It is a promising method to fabricate tissue constructs, which provides a high degree of control on construct design parameters essential for bone tissue regeneration, such as pore size, interconnectivity, filament diameter, degradation rate, and mechanical properties¹⁹. However, the 3D printing systems required to produce bone tissue-mimicking devices that support tissue growth are generally expensive, creating a barrier to widespread implementation, especially in laboratories with limited resources²⁰.

In this context, several studies have been conducted to investigate the potential of composite hydrogels composed of alginate and hydroxyapatite for biomedical applications. These hydrogels are printed on 3D scaffolds. The results have shown that the incorporation of hydroxyapatite into alginate-based hydrogels leads to increased secretion of type X collagen and promotes mineral deposition by chondrocytes within the composite hydrogel. These outcomes, in comparison to controls consisting solely of alginate, highlight the promising nature of the alginate/hydroxyapatite composite hydrogel for the formation of calcified cartilage and its suitability for 3D bioprinting^{21,22}.

As aforementioned, it is known that alginate combined with HAp can become a material with enormous potential for application in tissue engineering and 3D bioprinting. Therefore, the objective of this study was to fabricate alginate scaffolds with varying proportions of HAp using 3D printing technology. To overcome the limitations, associated with conventional and commercially available systems, a conventional filament 3D printer was modified and optimized for this purpose. The fabricated scaffolds were subjected to qualitative and quantitative analysis to evaluate their morphological characteristics, hydrophilicity, thermal and spectroscopic properties. Additionally, the biological response of the scaffolds was investigated through cell viability and cytotoxicity assays.

2. Experimental

2.1. Preparation of alginate/HAp scaffolds

2.1.1. Preparation of composite solution

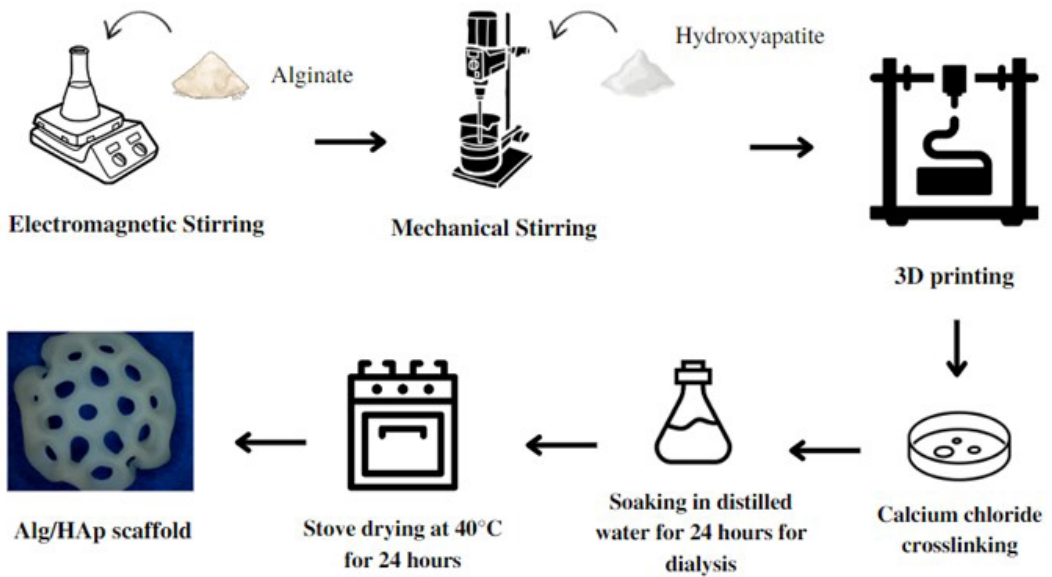
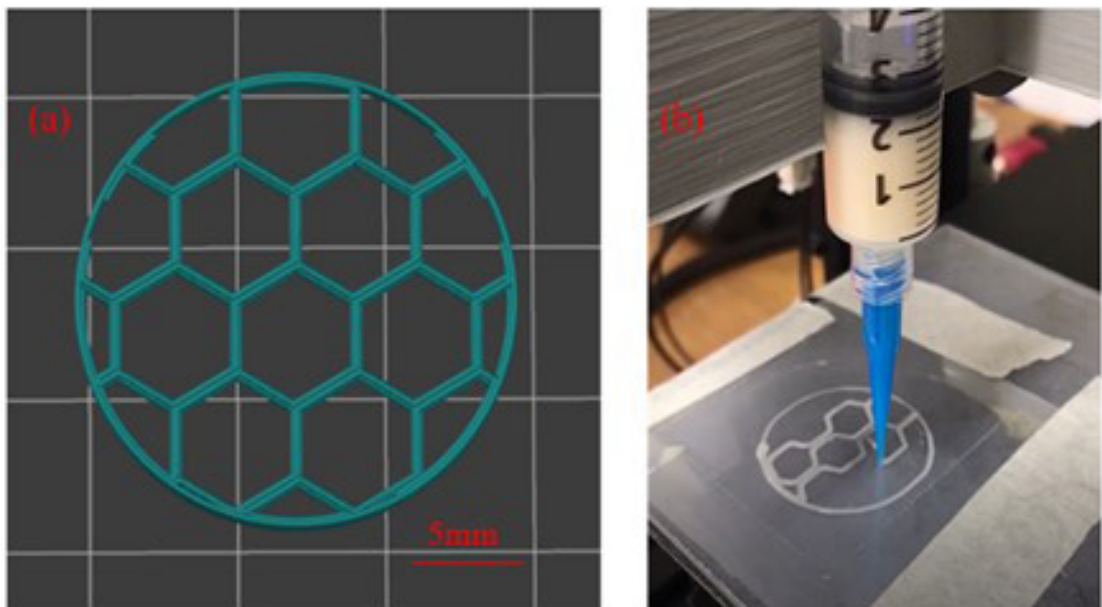
Initially, it was prepared a sodium alginate solution (Cromoline Química Fina, $M_v = 85.000 \text{ g/mol}$) at a concentration of 3.0% (w/v) in distilled water at 25°C using electromagnetic stirring for 3 hours. After printing attempts, it was noticed that it would be necessary to increase the alginate concentration to optimize the printability of the solution due to the low viscosity. The samples were then prepared in the same way, however, with concentrations of 5.0, 7.0, and 10.0% (w/v), and the latter ideal for use in printing the scaffolds. HAp (nanoXIM.HAp202, FLUIDINOVA, S.A, spherical nanoHA microaggregates with an average particle size of 5 μm) was added to this solution by mechanical stirring for 3 hours, at concentrations of 2.5 and 5.0% (w/v)³.

2.1.2. Design and extrusion of scaffolds

The modeling of the scaffolds was carried out using PrusaSlicer software, which allows the control of process parameters such as speed, extrusion force, internal filling, and filling pattern. The models have a diameter of 20mm, a layer height of 0.2mm, an internal filling of 20%, and "hexagonal" filling patterns. After modeling, the scaffolds were manufactured using a Bioender (Bioedtech). Table 1 presents the parameters used in the manufacture of scaffolds. Some adjustments were necessary due to the difference in printability presented with the presence of hydroxyapatite. In this way, the parameters were tested and optimized according to the morphology presented by the scaffolds. After printing, the scaffolds remaining for 24 hours at 25°C in a container containing 1.0, 2.5, and 5.0% (w/v) of calcium chloride (Vetec Química Fina, $M = 110,99 \text{ g/mol}$). The concentration of calcium chloride in the crosslinking did not show morphological and hydrophilic changes in the samples. Therefore, the smallest concentration of 1.0% (w/v) became the standard. After crosslinking, the scaffolds were immersed in distilled water for 24 hours at room temperature for dialysis. All samples were dried by conventional oven drying for 24 hours at 40°C. A schematic representation of the scaffold synthesis was presented in Figure 1. The models and bioprinting processes are exemplified in Figure 2. Three scaffolds compositions were produced: Alg (control), AlgHAp2.5, and AlgHAp5.0, where 2.5, and 5.0 correspond to the HAp concentrations.

Table 1. Printing parameters used in the scaffolds synthesis.

PARAMETERS	Alg	AlgHAp2.5	AlgHAp5.0
Extruder speed (mm/s)	8	7	7
Number of layers	5	5	5
Nose size (mm)	0.4	0.4	0.4
Setup Temperature (°C)	25	25	25
Extrusion multiplier	0.45	0.45	0.45
Extruder diameter (filament diameter) (mm)	1.55	1.55	1.55
Retraction length (mm)	7	5	5
Retraction Speed (mm/s)	9	15	15

**Figure 1.** Schematic representation of the alginate-based scaffold synthesis.**Figure 2.** (a) Scaffold model obtained through slicing software, and (b) 3D bioprinting process.

2.2. Characterization of AlgHAp scaffolds

2.2.1. Morphology

The morphological analysis was conducted with the scaffolds swollen and dried using a stereo microscope (ZEISS Stereo Discovery.V8), aiming at comparing the proportions of hydroxyapatite and investigating the parameter of the bioprinting process.

2.2.2. Swelling behavior

The gravimetric method assessed the hydrophilic property by determining the degree of swelling (Q) as a function of time, using distilled water as the swelling medium. To determine the Q values, the dry hydrogels were weighed (M_s) on an analytical balance (Shimadzu AUY-220) and subsequently immersed into 20mL of distilled water. After predetermined times, the hydrogels were removed from the swelling medium and weighed again (M_t). Q values were determined in g/g (gram of water per gram of hydrogel), according to Equation 1²⁰:

$$Q = \frac{M_t}{M_s} \quad (1)$$

2.2.3. Thermogravimetric analysis (TG) and differential thermogravimetric analysis (DTG)

Thermogravimetric analysis (TGA) was conducted on a TA Instruments SDT Q600 analyzer and was used to obtain information on the thermal degradation of materials. Samples of 8 mg were heated from 25 to 900 °C under a nitrogen atmosphere at a flow rate of 100 mL/min. All experiments were conducted at 10 °C/min to record thermogravimetric and derivative (TG/DTG) curves²⁰.

2.2.4. Chemical Characterization by Fourier transform infrared spectroscopy (FTIR) Spectroscopy

FTIR was used to characterize the presence of specific chemical groups in the AlgHAp samples. For this, the constituents of the scaffolds and the dry scaffolds were macerated, mixed with potassium bromide (KBr), and pressed at high pressure to obtain the tablet. The measurement was performed using transmission mode with investigated spectral range from 4000 to 400 cm^{-1} accumulating 128 scans with resolutions of 2cm^{-1} . The spectra were obtained using a Nicolet-NUXUS 610 FTIR spectrometer²⁰.

2.3. Cytotoxicity and cell viability assay

Cell viability and cytotoxicity of the alginate/hydroxyapatite scaffolds were assessed in triplicate by incubating them for 28 days in Dulbecco's Modified Eagle's Medium (DMEM) supplemented with 10% fetal bovine serum (Sigma-Aldrich). No medium change occurred during the incubation period. Benign canine mammary cells (E20) were directly seeded onto 24-well culture plates at a density of $5 \cdot 10^4$ cells per well and incubated at 37°C with 5% CO_2 for 48 hours. Following this period, the culture medium was removed from each well and replaced with fresh medium, without supplementation, for an additional 24 hours.

Subsequently, the culture medium was replaced with extracts obtained from the incubation of the scaffolds. After another 24 hours, the scaffold extracts were collected, and cell viability was assessed using the methylthiazolotetrazolium bromide (MTT) assay. The aliquots of these solutions were collected and incubated at 37°C with 5% CO_2 for 3 hours. Afterward, their absorbances were measured at 540 nm using a Multiskan FC (Thermo Scientific) instrument. Statistical analysis was conducted using one-way ANOVA with a Tukey's post hoc test in GraphPad Prism 8. Statistical significance was determined at p-values less than 0.05²¹.

3. Results and Discussion

3.1. Scaffolds characterization

3.1.1. Morphological characterization

Figure 3 displays digital images of the dried and swollen scaffolds, illustrating that the model's shape remained unchanged after the crosslinking process, even following swelling. The samples exhibited well-bonded and smooth surfaces, with a whitish color proportional to the amount of HAp present. The inclusion of HAp, regardless of the proportion, resulted in better printability of the samples. The original measurements of the project and the samples indicated that the swollen scaffold diameter was reduced by approximately 55% compared to the model's diameter. Additionally, the dry diameter exhibited a reduction of approximately 65%, regardless of the HAp proportion.

3.1.2. Swelling behavior

The swelling behavior was evaluated by measuring the weight of the samples over time, aiming to analyze the swelling kinetics, as shown in Figure 4. Optimized scaffold hydrogels should exhibit appropriate medium/water absorption^{22,23}. Swelling analysis can provide insight into the water and nutrient absorption capacity of a hydrogel. Our findings indicate that the samples exhibited similar behavior, with swelling equilibrium achieved after 5 hours, independently of the HAp proportion^{3,20,24}. The swelling degree values and time until equilibrium presented are compatible with scaffolds produced via natural polymer bioprinting or with hydroxyapatite reinforcements^{22,23}.

3.1.3. Thermogravimetric analysis (TG) and differential thermogravimetric analysis (DTG)

Figures 5 and 6 depict the TG and DTG curves of HAP, Alg, and their composites. Alginate-based scaffolds exhibited a typical first thermal event in the region of 100°C, which may be attributed to the vaporization of absorbed water on the sample surface. These samples also exhibited a second thermal event between 200 – 310°C, attributed to the onset of degradation and decomposition of the carbonaceous structure. A third thermal event observed between 360 – 530°C was attributed to complete matrix decomposition and subsequent formation of sodium carbonate (Na_2CO_3) through the recombination of thermally stable elements in this temperature range. Lastly, a fourth event was observed above 600°C, which may be related to non-elementary decomposition of Na_2CO_3 ²⁰.

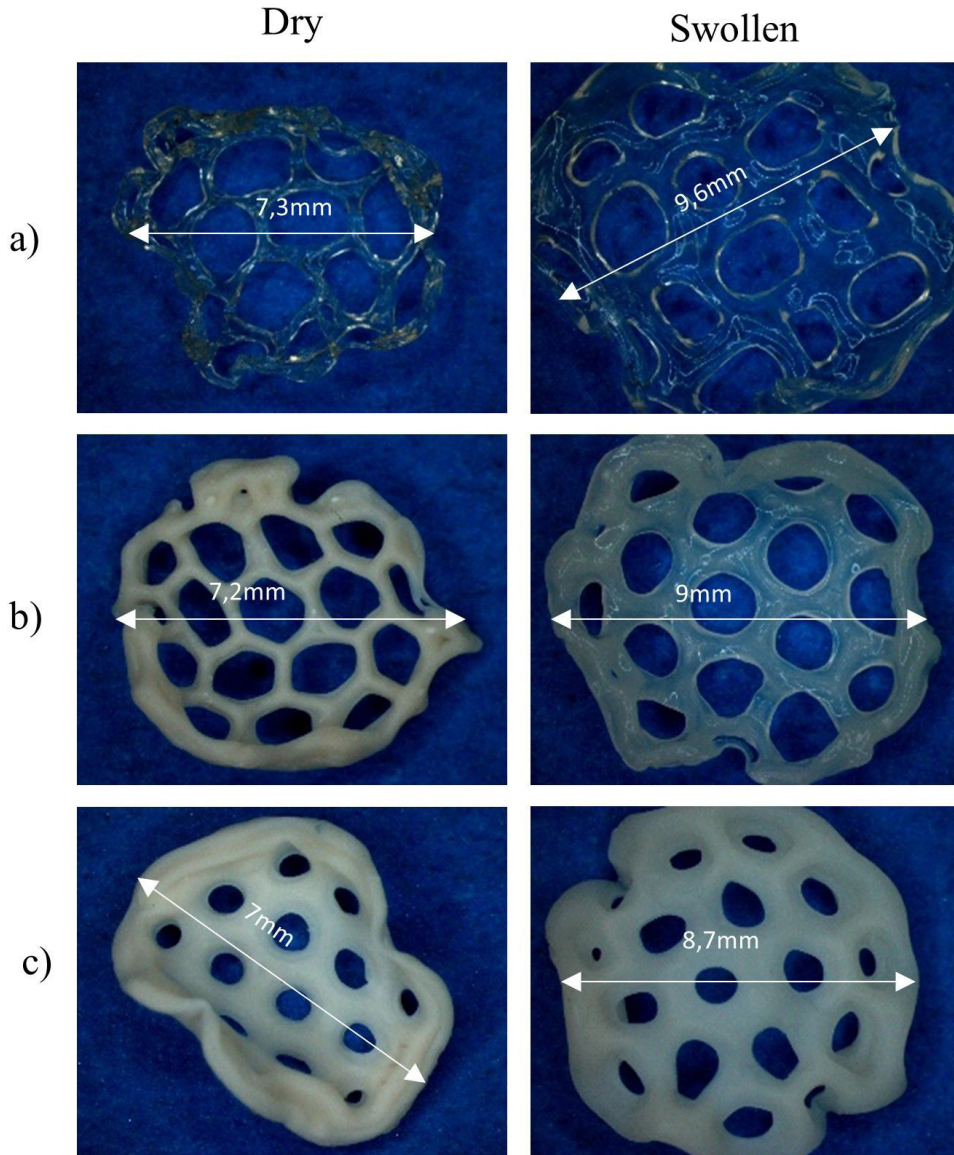


Figure 3. Dry and swollen scaffolds: a) Alg (control); b) AlgHAp2.5; c) AlgHAp5.0.

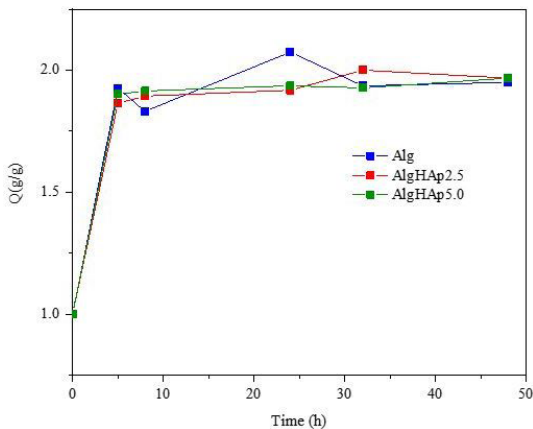


Figure 4. Dependence on the swelling degree by time of alginate and alginate-HAp composites.

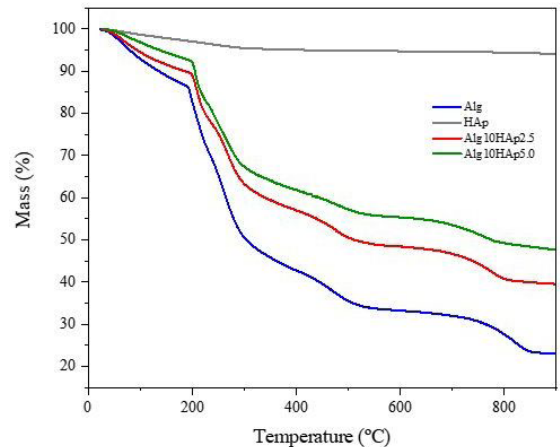


Figure 5. TG curves of pure HAp, Alg, Alg-HAp composites.

In pure HAp, a similar thermal event up to 100°C associated with the loss of physically adsorbed water molecules was also observed. The second thermal event between 250 – 600°C could be attributed to the loss of adsorbed carbonated molecules. The final event after 600°C is associated with the slow loss of lattice water^{25,26}.

The inclusion of HAp in the scaffolds did not considerably affect thermal stability, resulting in only a slight elevation of the initial degradation (T_i) temperature of the second thermal event. For instance, T_i values for Alg, AlgHAp2.5, and AlgHAp5.0 scaffolds were 186, 192, and 190°C, respectively. It was also noticed that the residue after the heating cycle increased with the increase in the amount of HAp, as expected.

3.1.4. Fourier transform infrared spectroscopy (FTIR)

The FTIR spectra of the hydrogels are shown in Figure 7, revealing their chemical composition. Alg hydrogel displayed characteristic alginate bands such as the asymmetric and symmetric stretchings of carboxylic group (COO⁻) at 1620 and 1414 cm⁻¹, respectively. The broad band observed from 3200 to 3600 cm⁻¹ in all spectra could be assigned to intramolecular and intermolecular O-H stretchings. The FTIR spectra of AlgHAp exhibited bending and stretching vibrations related to the phosphate group (PO₄³⁻) at 1020 and 605 cm⁻¹ coming from HAp, respectively. Furthermore, the intensity of these bands increased with an increase in the HAp content, confirming the formation of hydrogels and the incorporation of hydroxyapatite in the alginate matrix. No suppression or displacement of the composites bands was observed, indicating that the HAp-hydrogel interaction is weak. Table 2 summarizes the relevant spectroscopic absorption bands identified in the analysis^{3,20}.

3.2. Cytotoxicity and cell viability assay

The MTT assay was conducted in triplicate to evaluate cell viability. After 24 hours of incubation in the DMEM medium, the Alg and AlgHAp5.0 samples exhibited viability indexes exceeding 70% (Figure 8), indicating no significant decrease in cell viability compared to the benign canine mammary cells, E20 (control group). In the case of AlgHAp2.5 samples, the viability index are inside cytotoxicity limit (66.4 ± 7.0%). AlgHAp5.0% displayed cell viability values exceeding 100%, suggesting that the scaffolds are non-cytotoxic for the investigated cell lineage and may promote cell proliferation. These preliminary findings will be further complemented with additional data in future research.

Table 2. Main absorption bands observed from FTIR technique.

WAVENUMBER (cm ⁻¹)	FUNCTIONAL GROUPS
3200-3600	Stretching of hydroxyl group (-OH)
1620 and 1414	Asymmetric and symmetric stretchings of carboxylic groups (-COO ⁻)
892	Stretching of ether groups C-O-C
1020	Bending of P-O present in PO ₄ ³⁻
605	Stretching of P-O present in PO ₄ ³⁻

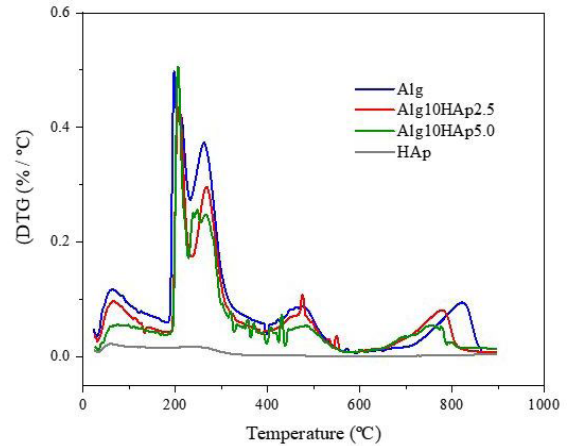


Figure 6. DTG curves of pure HAp, Alg, Alg-HAp composites.

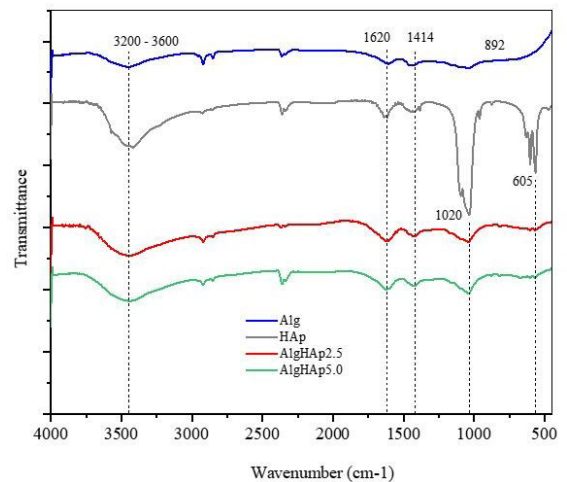


Figure 7. FTIR spectra of pure HAp, Alg, Alg-HAp composites.

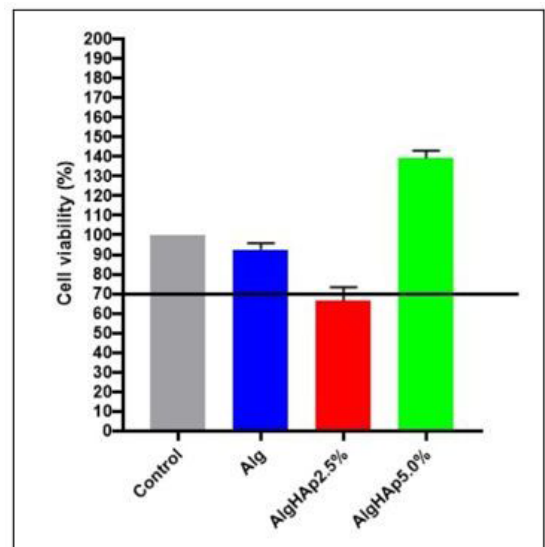


Figure 8. Cell viability of pure HAp, Alg, Alg-HAp composites.

4. Conclusions

Based on the results obtained, it can be inferred that the development of alginate scaffolds with hydroxyapatite reinforcements using a 3D bioprinter is feasible and shows good reproducibility through modeling in slicing software. The analyzes indicate that the swelling kinetics and the main morphological aspects were maintained, regardless of the hydroxyapatite concentration. From FTIR, it was possible to prove the formation of hydrogels, and the peaks of 1020 and 605 cm^{-1} demonstrate the incorporation of hydroxyapatite in the alginate matrix. Thermal analysis demonstrates that HAp slight improves the thermal stability of the scaffolds. The results showed the promising potential of alginate as a composite matrix, offering the ability to integrate important properties for bone regeneration through the incorporation of hydroxyapatite, preserving the fundamental characteristics of alginate. Furthermore, the scaffolds are not cytotoxic to the cell line studied and can help cell proliferation.

5. Acknowledgements

The authors would like to thank to the Sao Paulo State University (UNESP), São Paulo Research Foundation (FAPESP) (2018/18697-1; 2013/03643-0; 2013/07296-2), National Council for Scientific and Technological Development (CNPq) (MRM 315513/2021-7; FAA 312414/2018-8; 316174/2021-1; MCTIC Grant #406973/2022-9 through INCT/Polysaccharides – National Technology-Science Institute for Polysaccharides). This study was financed in part by the Coordenação de Aperfeiçoamento de Pessoal de Nível Superior – Brasil (CAPES) – “Finance Code 001”.

6. References

- Tortora GJ, Derrickson B. Principles of anatomy & physiology. Porto Alegre: Artmed; 2012.
- Seo S-J, Mahapatra C, Singh RK, Knowles JC, Kim H-W. Strategies for osteochondral repair: focus on scaffolds. *J Tissue Eng.* 2014;5:1-14.
- Barros J, Ferraz MP, Azeredo J, Fernandes MH, Gomes PS, Monteiro FJ. Alginate-nanohydroxyapatite hydrogel system: optimizing the formulation for enhanced bone regeneration. *Mater Sci Eng C.* 2019;105:109985.
- Parhi P, Ramanan A, Ray AR. Preparation and characterization of alginate and hydroxyapatite-based biocomposite. *J Appl Polym Sci.* 2006;102:5162-5.
- Tozzi G, Mori A, Oliveira A, Roldo M. Composite hydrogels for bone regeneration. *Materials.* 2016;9(4):267-91.
- Birt MC, Anderson DW, Toby EB, Wang JX. Osteomyelitis: recent advances in pathophysiology and therapeutic strategies. *J Orthop.* 2017;14:45-52.
- Zhang X, Yin X, Luo J, Zheng X, Wang H, Wang J et al. Novel hierarchical nitrogen-doped multiwalled carbon nanotubes/cellulose/nanohydroxyapatite nanocomposite as an osteoinductive scaffold for enhancing bone regeneration. *ACS Biomater Sci Eng.* 2019;5:294-307.
- Hupp JR. Wound repair. In: Peterson LJ, editor. Contemporary oral and maxillofacial surgery. 4th ed. St. Louis: The CV Mosby Co; 2004. p. 55-62.
- Junqueira LC, Carneiro J. Histologia básica. 11th ed. Rio de Janeiro: Guanabara Koogan; 2011. Chapter 8, Tecido ósseo; p. 135-52.
- Luo Y, Lode A, Wu C, Chang J, Gelinsky M. Alginate/nanohydroxyapatite scaffolds with designed core/shell structures fabricated by 3D plotting and in situ mineralization for bone tissue engineering. *ACS Appl Mater Interfaces.* 2015;7(12):6541-9.
- Ribeiro M, Moraes MA, Beppu MM, Garcia MP, Fernandes MH, Monteiro FJ et al. Development of silk fibroin/nanohydroxyapatite composite hydrogels for bone tissue engineering. *Eur Polym J.* 2015;67:66-77.
- Costa HS, Dias MR. Alginate/bioactive glass beads: synthesis, morphological and compositional changes caused by SBF immersion method. *Mater Res.* 2021;24(4):e20200587.
- Obara S, Yamauchi T, Tsubokawa N. Evaluation of the stimulus response of hydroxyapatite/calcium alginate composite gels. *Polym J.* 2010;42:161-6.
- Turco G, Marsich E, Bellomo F, Semeraro S, Donati I, Brun F et al. Alginate/hydroxyapatite biocomposite for bone ingrowth: a trabecular structure with high and isotropic connectivity. *Biomacromolecules.* 2009;10:1575-83.
- Chen L, Shen R, Komasa S, Xue Y, Jin B, Hou Y et al. Drug-loadable calcium alginate hydrogel system for use in oral bone tissue repair. *Int J Mol Sci.* 2017;18(5):989.
- Abreu FOMS, Bianchini C, Forte MMC, Kist TBL. Influence of the composition and preparation method on the morphology and swelling behavior of alginate chitosan hydrogels. *Carbohydr Polym.* 2008;74:283-9.
- Sarker B, Singh R, Silva R, Roether JA, Kaschta J, Detsch R et al. Evaluation of fibroblasts adhesion and proliferation on alginate-gelatin crosslinked hydrogel. *PLoS One.* 2014;9:e107952.
- Vural AC, Odabas S, Korkusuz P, Sağlam ASY, Bilgiç E, Çavuşoğlu T et al. Cranial bone regeneration via BMP-2 encoding mesenchymal stem cells. *Artif Cells Nanomed Biotechnol.* 2017;45:544-50.
- Moncal KK, Heo DN, Godzik KP, Sosnoski DM, Mrowczynski OD, Rizk E et al. 3D printing of poly(ϵ -caprolactone)/poly(D,L-lactide-coglycolide)/hydroxyapatite composite constructs for bone tissue engineering. *J Mater Res.* 2018;33:1972-86.
- Kahl M. Ultra-low-cost 3D bioprinting: modification and application of an off-the shelf desktop 3D-printer for biofabrication. *Front Bioeng Biotechnol.* 2019;7:184.
- You F, Chen X, Cooper DML, Chang T, Eames BF. Homogeneous hydroxyapatite/alginate composite hydrogel promotes calcified cartilage matrix deposition with potential for three-dimensional bioprinting. *Biofabrication.* 2019;11:015015.
- Liu S, Hu Y, Zhang J, Bao S, Xian L, Dong X et al. Bioactive and biocompatible macroporous scaffolds with tunable performances prepared based on 3D printing of the pre-crosslinked sodium alginate/hydroxyapatite hydrogel ink. *Macromol Mater Eng.* 2019;304:1800698.
- Fernandes RS. Desenvolvimento de hidrogéis bionanocompósitos ativos baseados em amido e alginato com potencial aplicação na agricultura e na biomedicina [thesis]. Ilha Solteira: Universidade Estadual Paulista “Júlio de Mesquita Filho”; 2020.
- Chakraborty J, Majumder N, Sharma A, Prasad S, Ghosh S. 3D bioprinted silk-reinforced Alginate-Gellan Gum constructs for cartilage regeneration. *Bioprinting.* 2022;28:e00232.
- Souza D. Biocompósitos eletrofiados de PLLA com alto conteúdo de partículas de fosfato de cálcio funcionalizados para regeneração óssea [thesis]. São Paulo: Universidade de São Paulo; 2017.
- Palacios J, Albano C, González G, Castillo RV, Karam A, Covis M. Characterization and thermal degradation of poly(ϵ -lactide-co-glycolide) composites with nanofillers. *Polym Eng Sci.* 2013;53:1414-29.